

Comparison Between Protein-Protein Interaction Networks CD4$^+$T and CD8$^+$T and a Numerical Approach for Fractional HIV Infection of CD4$^+$T Cells

Eslam Farsimadan(✉), Leila Moradi, Dajana Conte, Beatrice Paternoster, and Francesco Palmieri

University of Salerno, 84084 Fisciano, Italy
{efarsimadan,lmoradi,dajconte,beapat,fpalmieri}@unisa.it

Abstract. This research examines and compares the construction of protein-protein interaction (PPI) networks of CD4$^+$ and CD8$^+$T cells and investigates why studying these cells is critical after HIV infection. This study also examines a mathematical model of fractional HIV infection of CD4$^+$T cells and proposes a new numerical procedure for this model that focuses on a recent kind of orthogonal polynomials called discrete Chebyshev polynomials. The proposed scheme consists of reducing the problem by extending the approximated solutions and by using unknown coefficients to nonlinear algebraic equations. For calculating unknown coefficients, fractional operational matrices for orthogonal polynomials are obtained. Finally, there is an example to show the effectiveness of the recommended method. All calculations were performed using the Maple 17 computer code.

Keywords: Protein-protein interaction network · HIV infection of CD4$^+$T · Discrete Chebyshev polynomials · Fractional calculus · Absolute errors

1 Introduction

A lentivirus, the human immunodeficiency virus (HIV), causes acquired immunodeficiency syndrome (AIDS). HIV infection is distinguished by alterations in the function of T cells and homeostasis and the extreme heterogeneity between infected people and those untreated. On average, most patients infected with HIV develop AIDS in 10 to 20 years. Variations in HIV infection clinical outcomes may be due to genetic differences in HIV strains, host genetic differences, or differences in virus-specific inflammatory responses. The first HIV case was confirmed in 1980. Due to the latest count, more than 35 million people have died as a result of HIV, and over 37 million people have this virus in their bodies, posing a threat to the rest of the world. They will also convey this danger by mother-to-child transfer, unsafe sex, and other ways.

© Springer Nature Switzerland AG 2021
O. Gervasi et al. (Eds.): ICCSA 2021, LNCS 12949, pp. 78–94, 2021.
https://doi.org/10.1007/978-3-030-86653-2_6

There have already been several mathematical models developed to research the within-host dynamics of HIV infection [4,19,30]. Virus-to-cell infection was the focus of the majority of these models. Direct cell-to-cell transmitting is also a possibility for the virus to spread. An ODE model of HIV virus spread in a well-mixed compartment like the bloodstream, was proposed by Perelson [23,24]. Within the field of mathematical modeling of HIV infection, this model has had a noteworthy effect. Other several approaches have been suggested based on Perelson model [1,3,8,10,11,13,16,21,26,29,31]. However, most HIV infection modeling research has focused on integer-order ordinary differential equations [5,14,22,32].

Fractional calculus (FC) has recently been widely used in a variety of fields. Plenty of applied scientists and mathematicians have attempted to use fractional calculus to model real-world processes. Fractional kinetics in complex systems, reported in [17]. The dynamics of the fractional-order in botanical impedances were studied in [12]. A mathematical fractional-order model of human root dentin was presented in [25].

In biology, it has been determined that biological organisms' cell membranes have fractional-order electrical conductance, which is then categorized into non-integer order models. Fractional derivatives represent basic characteristics of cell-rheological conduct and have had the best achievement in the area of rheology [7]. Furthermore, it has been demonstrated that the behavior modeling by fractional ordinary differential equations (FODE) for the vestibule oculomotor neurons has more benefits than the classical integer-order modeling [2]. FODE is intrinsically linked to systems found in all biological systems. They are also associated with fractals, which are normally found in biological systems. In this study, we propose a FODE system for modeling HIV and a numerical method for solving it.

The following is the paper's structure. The primary objective of selecting FODE for modeling HIV infection of CD4$^+$T cells is described in Sect. 2. In fact, in this section, we present and compare the protein-protein interaction network of cell infection. In Sect. 3, the mathematical model will be outlined. The formulation of the DCPs and their properties are covered in Sect. 4. The numerical solution of HIV infection of CD4$^+$T cells is discussed in Sect. 5. Section 6, describes illustrative examples that show the DCP's superiority. Finally, in Sect. 7, the main concluding remark is summarized.

2 Comparison Protein-Protein Interaction Networks CD4$^+$T and CD8$^+$T

CD4$^+$T lymphocytes are a kind of white blood cell as well as a lymphocyte. A helper T cell is also known as a T cell that assists other cells. CD4$^+$T cells primarily serve as a type of T cell that helps other T cells resist virus infection, while CD8$^+$ cells are widely distributed on the surface of suppressor and cytotoxic T lymphocytes during HIV infection. The researchers concluded that HIV infection caused severe immune system problems, including the loss of CD4$^+$T cells and a reduction in the $\frac{CD4^+}{CD8^+}$T cell ratio.

In the peripheral group of healthy adults, the $\frac{CD4^+}{CD8^+}$T ratio is about 2:1, and an abnormal ratio may signify disorders related to autoimmunity or immunodeficiency. An inverted $\frac{CD4^+}{CD8^+}$T ratio (i.e., less than $\frac{1}{1}$) means that the immune system is compromised. As a result, it is critical to look into the differences between $CD4^+$ and $CD8^+$T cells at various stages of HIV infection.

AIDS is caused by the pathogen HIV, which is well-known. The researchers reasoned that analyzing the differences in mutual differentially expressed genes between $CD4^+$ and $CD8^+$Tcells at different phases of disease would reveal more about HIV.

Few studies examine the systemic features of $CD4^+$T cells at various levels of HIV infection or the differences between $CD4^+$ and $CD8^+$T cells at the same level. And this topic is beyond the scope of this article's discussion. In this study, we simply compare and contrast the construction of protein-protein interaction (PPI) networks in $CD4^+$ and $CD8^+$T cells after HIV infection. We investigate the overlapping differentially expressed genes in $CD4^+$ cells and those in $CD8^+$T cells in two PPI networks and compare two PPI networks Fig. 1, to comprehend the differentially expressed between $CD4^+$ and $CD8^+$ from a network perspective.

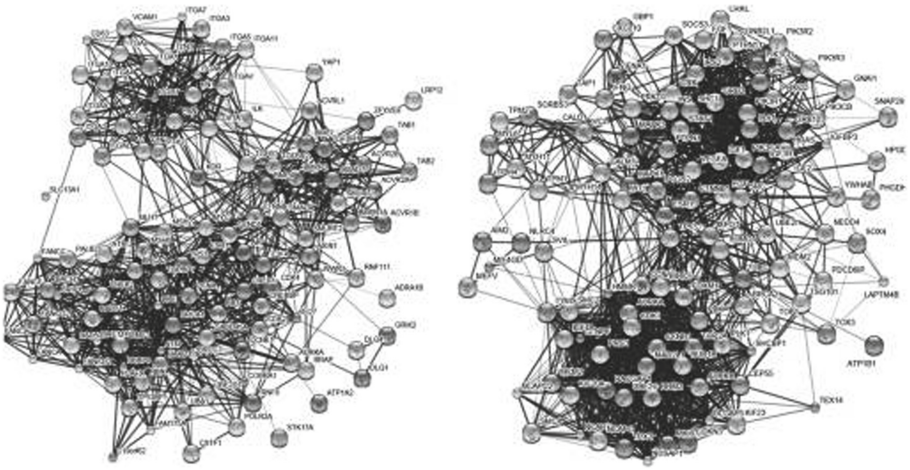

Fig. 1. PPI network constructed in $CD8^+$T cells (right) and $CD4^+$T cells (left)

The amount of overlapping of different expressed genes in each cell type is extremely high, and the two PPI networks shown in Fig. 1 are far too convoluted to provide significant network information. As a result, we compare the functional modules from each PPI network in separate networks to assess the differences between two HIV-infected cells, respectively (Figs. 2, 3). The immune responses of $CD4^+$ and $CD8^+$T cells at various stages after HIV infection are diverse, as shown in Figs. 2, 3.According to research, specific $CD8^+$T cells play a

key role in directly combating HIV infection, while CD4$^+$T cells primarily serve to support CD8$^+$T cells.

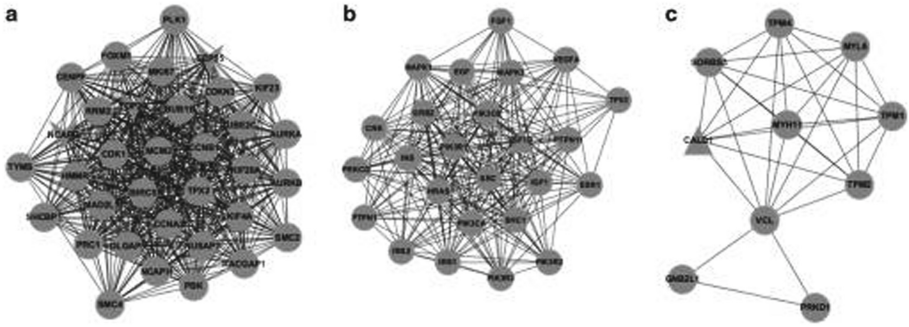

Fig. 2. (a-c) Function modules obtained by the PPI network in CD8$^+$T cells.

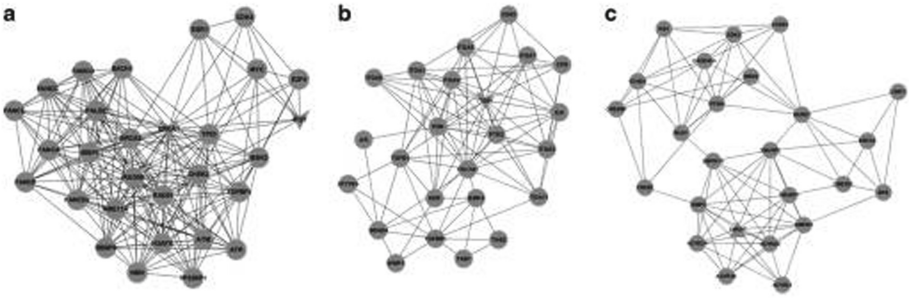

Fig. 3. (a-c) Functional modules obtained by the PPI network in CD4$^+$T cells.

It has been validated by comparing networks and prior research that CD4$^+$T cells undergo gradual depletion after HIV infection and that virus reproduction (more than 99 %) happened primarily in CD4$^+$T cells in the peripheral blood and lymphoid tissue. HIV infection can also stop CD4$^+$T cells from proliferating. As a consequence, HIV is a retrovirus that primarily infects CD4$^+$T cells. CD4$^+$T cells will develop new virions after being infected, leading to more cell infection and viral development (See Fig. 4). Therefore, for researchers, studying these cells is critical. We want to introduce a mathematical model of fractional HIV infection of CD4$^+$T cells and find a numerical solution for it in this work.

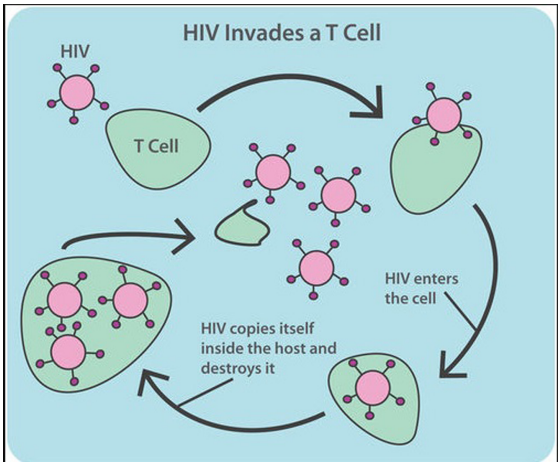

Fig. 4. HIV virus invades Tcell.

3 Mathematical Model Information

In the following, definitions of the Caputo and Riemann-Liouville fractional integral and derivative are discussed [20,28].

Definition 1. *Let $\alpha > 0$. The Riemann-Liouville fractional integration of order α is defined as*

$$\left(\mathbf{I}^{\alpha}\mathrm{f}\right)(t) = \begin{cases} \dfrac{1}{\Gamma(\alpha)} \displaystyle\int_0^t \dfrac{\mathrm{f}(z)dz}{(t-z)^{1-\alpha}}, & \alpha > 0, \\ \mathrm{f}(t), & \alpha = 0. \end{cases}$$

Definition 2. *Let $\alpha > 0$ and n is an integer. The Caputo fractional derivative of order α, is described as*

$$\mathbf{D}^{\alpha}\mathrm{f}(t) = \begin{cases} \dfrac{1}{\Gamma(n-\alpha)} \displaystyle\int_0^t \dfrac{\mathrm{f}^{(n)}(z)}{(t-z)^{\alpha-n+1}}dz, \ t > 0, & 0 \le n-1 < \alpha < n, \\ \dfrac{d^n \mathrm{f}(t)}{dt^n}, & \alpha = n \in \mathtt{N}. \end{cases}$$

Now we present the HIV infection model in CD4$^+$T cells with fractional-order. The following FODE is used to characterize the new system:

$$\begin{aligned} &\mathbf{D}^{\alpha}T = q - \eta T + rT\left(1 - \tfrac{T+1}{T_{\max}}\right) - kVT, \\ &\mathbf{D}^{\alpha}I = kVT - \beta I, \\ &\mathbf{D}^{\alpha}V = \mu\beta I - \gamma V, \end{aligned} \tag{1}$$

where $T(0) = r_1,\ I(0) = r_2,\ V(0) = r_3,\ 0 \le t \le R < \infty$.

Where $V(t)$, $I(t)$, and $T(t)$ represent free HIV particles within the blood, CD4$^+$T cells contaminated by HIV, and the concentration of susceptible CD4$^+$T cells, respectively. R is any positive constant. The terms η, γ, and β indicate the normal circulation rates of non-infected T cells, virus particles, and infected T cells, respectively. $1 - \frac{T+1}{T_{\max}}$ depicts the logistic growth of healthy CD4$^+$T cells while ignoring the proliferation of infected CD4$^+$T cells. The term KVT reflects the occurrence of HIV infection of healthy CD4$^+$T cells when $k > 0$ is the infection rate. During its lifetime of CD4$^+$T cell, each infected CD4$^+$T cell is expected to generate l virus particles. The body is attempted to make CD4$^+$T cells at a constant rate q from precursors in the bone marrow and thymus. Whenever T cells are stimulated by antigen or mitogen, they multiply at a rate of r via mitosis. The maximum CD4$^+$T cell concentration in the body is denoted by $T_{\max}$.

4 Preliminary Remarks

4.1 Discrete Chebyshev Polynomials

We will focus our attention in this section on the fundamental definition, formulation, and characteristics of a large family of orthogonal polynomials namely discrete Chebyshev polynomials introduced by P.L. Chebyshev [9,18].

Definition 3. *The discrete Chebyshev polynomials $\mathcal{C}_{n,N}(x)$ are defined as*

$$\mathcal{C}_{n,N}(x) = \sum_{k=0}^{n} (-1)^k \binom{n+k}{n} \binom{N-k}{n-k} \binom{x}{k}, \quad n = 0, 1, ..., N, \tag{2}$$

where N be a positive integer number.

The discrete Chebyshev polynomials set $\{\mathcal{C}_{n,N}, n = 0, 1, ..., N\}$ are orthogonal on $[0, N]$ according to the following discrete norm:

$$\langle \mathrm{f}, \mathrm{g} \rangle = \sum_{r=0}^{N} \mathrm{f}(r)\mathrm{g}(r). \tag{3}$$

These polynomials have the following orthogonality property:

$$\langle \mathcal{C}_{m,N}, \mathcal{C}_{n,N} \rangle = \sum_{r=0}^{N} \mathcal{C}_{m,N}(r)\mathcal{C}_{n,N}(r) = \xi_n \delta_{mn},$$

where δ_{mn} is the Kronecker delta and ξ_n is introduced by the following relation:

$$\xi_n = \frac{(N+n+1)!}{(2n+1)(N-n)!(n!)^2}. \tag{4}$$

By using (2), the analytical form of $\mathcal{C}_{n,N}(t)$ can be obtained as:

$$\mathcal{C}_{n,N}(t) = \sum_{k=0}^{n} \mathsf{a}_{j,n} x^k, \quad n = 0, 1, ...N, \tag{5}$$

where

$$\mathsf{a}_{j,n} = \sum_{r=j}^{n} \frac{(-1)^r \binom{n+r}{n} \binom{N-r}{n-r} s(r,i)}{r!}. \tag{6}$$

and $s(r,i)$ is a Stirling numbers of the first kind [27].

4.2 Shifted Discrete Chebyshev Polynomials

We construct the shifted discrete Chebyshev polynomials (SDCPs) by changing the variable $x = Nt$ for using the discrete Chebyshev polynomials over $[0,1]$. Let nth SDCPs (i.e. $\mathcal{C}_{n,N}(Nt)$) to be marked by $\mathcal{S}_{n,N}(t)$. The set of SDCPs $\{\mathcal{S}_{n,N}, n = 0,1,...,N\}$ are then orthogonal on $[0,1]$ according to the discrete norm as follow:

$$\langle \mathrm{f}, \mathrm{g} \rangle_* = \sum_{r=0}^{N} \mathrm{f}\left(\frac{r}{N}\right) \mathrm{g}\left(\frac{r}{N}\right). \tag{7}$$

The property of orthogonality for SDCPs is described by:

$$\langle \mathcal{S}_{m,N}(t), \mathcal{S}_{n,N}(t) \rangle_* = \sum_{r=0}^{N} \mathcal{S}_{m,N}\left(\frac{r}{N}\right) \mathcal{S}_{n,N}\left(\frac{r}{N}\right) = \xi_n \delta_{mn}, \tag{8}$$

where ξ_n was introduced in (4).

Let $\mathrm{f}(t)$ defined on $[0,1]$. $\mathrm{f}(t)$ can be expanded by the SDCPs as follows:

$$\mathrm{f}(t) \simeq \sum_{i=0}^{N} c_i \mathcal{S}_{i,N}(t) = C^T \Psi(t), \tag{9}$$

where C and $\Psi(t)$ are $(N+1)$ vectores given by

$$C^T = [c_0, c_1, ..., c_N]^T, \tag{10}$$

$$\Psi(t) = [\mathcal{S}_{0,N}(t), \mathcal{S}_{1,N}(t), ..., \mathcal{S}_{N,N}(t)]^T, \tag{11}$$

and the coefficients c_i can be obtained by the following expression:

$$c_i = \frac{\langle \mathrm{f}(t), \mathcal{S}_{i,N}(t) \rangle_*}{\xi_i}, \quad i = 0,1,...N. \tag{12}$$

Operational Matrices:

In the follow-up, explicit formulas for operational matrices of Riemann-Liouville fractional integration for SDCPs are provided. In addition, the SDCPs vector's product operating matrix is calculated.

Lemma 1. *[15] The inner product of the $\mathcal{S}_{n,N}(t)$ and t^r, indicated by $\lambda(n,r)$, can be calculated for a positive integer r as follows:*

$$\lambda\left(n,r\right)=\frac{1}{N^r}\sum_{j=0}^{N}\sum_{k=0}^{n}\mathsf{a}_{j,n}j^{k+r}, \tag{13}$$

where $\mathsf{a}_{j,n}$ is introduced in (6).

Theorem 1. *[6,15] Assume that $\Psi(t)$ is the SDCPs vector specified in (11). Then, its Riemann-Liouville fractional integral of order α is*

$$\mathbf{I}^{\alpha}\Psi(t)=\mathcal{P}^{(\alpha)}\Psi(t), \tag{14}$$

where $\mathcal{P}^{(\alpha)}$ is fractional integral operational matrix and

$$\mathcal{P}_{i,j}^{(\alpha)}=\sum_{j=0}^{N}\left(\sum_{k=0}^{i}\frac{\mathsf{a}_{k,N}\lambda(k+\alpha,j)\alpha(k+1)}{\alpha(k+\alpha+1)}\right),\qquad i,j=1,2,...,N+1. \tag{15}$$

Theorem 2. *[6,15] Consider that $\Psi(t)$ is the SDCPs vector specified in (11) and Q be an arbitrary $(N+1)$ vector. Then*

$$\Psi(t)\Psi^{T}(t)Q=\tilde{Q}\Psi(t), \tag{16}$$

where $\tilde{Q}$ is the $(N+1)\times(N+1)$ product operational matrix and

$$\tilde{Q}_{i+1,j+1}=\frac{1}{\xi_j}\sum_{k=0}^{N}Q_k\left\langle\mathcal{S}_{k,N}(t)\mathcal{S}_{i,N}(t),\mathcal{S}_{j,N}(t)\right\rangle_{*},\quad i,j=0,1,...,N.$$

5 The Numerical Method

SDCPs are used to approximate the solution of fractional HIV infection of CD4$^+$T cells, In this section. Consider the FODE (1) and $\mathbf{D}^{\alpha}T(t),\mathbf{D}^{\alpha}I(t)$ and $\mathbf{D}^{\alpha}V(t)$ involved in, as follows:

$$\mathbf{D}^{\alpha}T(t)\simeq F^{T}\Psi(t),\ \ \mathbf{D}^{\alpha}I(t)\simeq G^{T}\Psi(t),\ \ \mathbf{D}^{\alpha}V(t)\simeq H^{T}\Psi(t), \tag{17}$$

where $\Psi(t)$ is the SDCPs vector specified in (11). Furthermore, F,G,H are unknown vectors that should be determined. By using of fractional Riemann-Liouville operator $\mathbf{I}^{\alpha}$, we have:

$$\begin{cases} T \simeq \mathbf{I}^{\alpha} F^T \Psi(t) + \sum_{k=0}^{m-1} T^{(k)}(0) \frac{t^k}{k!} = F^T \mathcal{P}^{(\alpha)} \Psi(t) + d_1 \Psi(t), \\ I \simeq \mathbf{I}^{\alpha} G^T \Psi(t) + \sum_{k=0}^{m-1} I^{(k)}(0) \frac{t^k}{k!} = G^T \mathcal{P}^{(\alpha)} \Psi(t) + d_2 \Psi(t), \\ V \simeq \mathbf{I}^{\alpha} H^T \Psi(t) + \sum_{k=0}^{m-1} V^{(k)}(0) \frac{t^k}{k!} = H^T \mathcal{P}^{(\alpha)} \Psi(t) + d_3 \Psi(t), \end{cases} \tag{18}$$

where $\mathcal{P}^{(\alpha)}$ is the fractional operational matrix of SDCPs vector derived in (14).

Substituting (17)–(18) in FODE (1), we have the following residual functions as:

$$\begin{cases} E_1(t) \simeq (F^T \Psi(t)) - q - \eta(F^T \mathcal{P}^{(\alpha)} \Psi(t) + d_1 \Psi(t)) + r(F^T \mathcal{P}^{(\alpha)} \Psi(t) + d_1 \Psi(t)) \\ (1 - \frac{(F^T \mathcal{P}^{(\alpha)} \Psi(t) + T(0)) + 1}{T_{\max}}) - k(H^T \mathcal{P}^{(\alpha)} \Psi(t) + d_2 \Psi(t))(F^T \mathcal{P}^{(\alpha)} \Psi(t) + d_1 \Psi(t)), \\ \\ E_2(t) \simeq (G^T \Psi(t)) - k(H^T \mathcal{P}^{(\alpha)} \Psi(t) + d_2 \Psi(t))(F^T \mathcal{P}^{(\alpha)} \Psi(t) + d_1 \Psi(t) + \\ \beta(G^T \mathcal{P}^{(\alpha)} \Psi(t) + d_3 \Psi(t)), \\ \\ E_3(t) \simeq (H^T \Psi(t)) - \mu\beta(G^T \mathcal{P}^{(\alpha)} \Psi(t) + d_3 \Psi(t)) + \gamma(H^T \mathcal{P}^{(\alpha)} \Psi(t) + d_2 \Psi(t)). \end{cases} \tag{19}$$

Now, to find the solution $T(t), I(t)$ and $V(t)$, we must first collocate the residual functions $E_i(t)$, $i = 1, 2, 3$ at the $N+1$ points. We use roots of shifted Chebyshev polynomials to find appropriate collocates, as shown below:

$$E_i(t_j) = 0, \quad i = 1, 2, 3, \ j = 1, 2, ...N + 1. \tag{20}$$

Solve the system of algebraic equations to achieve unknown coefficients of the vectors F, G, H. Finally, we obtain the numerical solution by inputting the acquired vectors F, G, H in Eq. (1).

6 Computational Results and Comparisons

The effectiveness of the shifted discrete chebyshev polynomials method for solving fractional HIV infection of CD4$^+$T cells is proved in this section. In the following, one example is given to demonstrate the properties of the new model.

- SDCPM = Shifted discrete chebyshev polynomials method
- All computations are carried out using MAPLE 17 with 16 digits precision

In the $t \in [0, 1]$, we used the described method for FODEs (1) with the initial conditions $T(0) = 0.1, I(0) = 0$, and $V(0) = 0.1$. $q = 0.1, \eta = 0.02, \beta = 0.3, r = 3, \gamma = 2.4, k = 0.0027, T_{max} = 1500, \mu = 10$ were used in this article.

Approximate solutions population of healthy CD4$^+$T cells, infected CD4$^+$T cells, and free HIV particle for $N = 8$ and different α in $[0, 1]$ are represented in Figs. 5, 6, and 7, respectively. Can be seen in Figs. 8, 9, and 10, that $T(t)$, the concentration of susceptible CD4$^+$T cells, increases rapidly, $I(t)$, the amount of

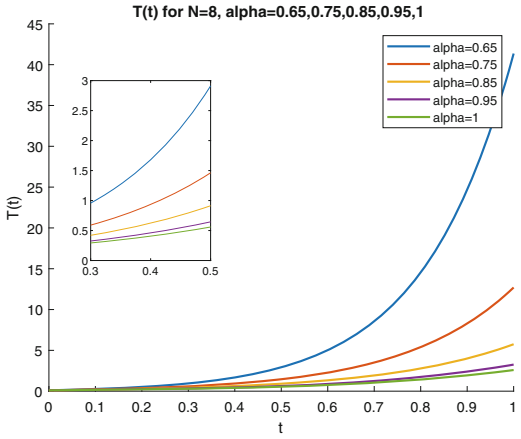

Fig. 5. Numerical results comparison $T(t)$ for $N = 8$ and different α in $[0, 1]$.

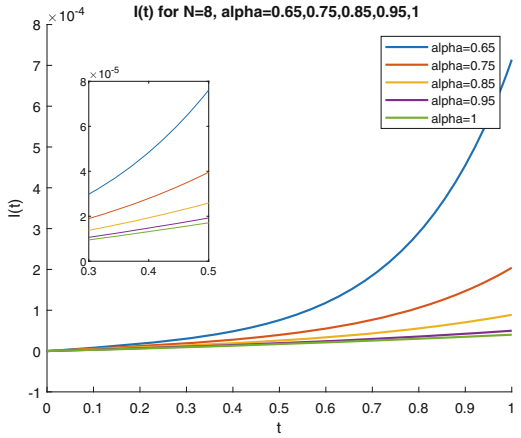

Fig. 6. Numerical results comparison $I(t)$ for $N = 8$ and different α in $[0, 1]$.

Table 1. Numerical results comparison for $T(t)$.

Method	$t = 0.2$	$t = 0.4$	$t = 0.6$	$t = 0.8$	$t = 1.0$
Runge-kutta [5]	0.208808	0.406240	0.764423	1.414046	2.591594
MVIM [14]	0.208808	0.406240	.764428	1.414094	2.208808
VIM [14]	0.208807	0.406134	0.762453	1.397880	2.506746
LADM-Pade [22]	0.208807	0.406105	0.761146	1.377319	2.329169
Bessel [32]	0.203861	0.380330	0.695462	1.275962	2.383227
SDCPM	0.208807	0.406240	0.764422	1.414045	2.591592

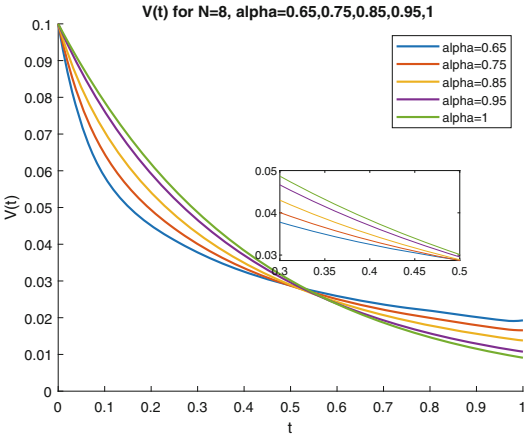

Fig. 7. Numerical results comparison $V(t)$ for $N = 8$ and different α in $[0, 1]$.

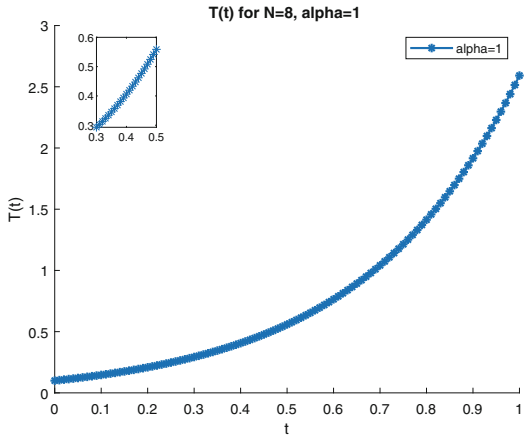

Fig. 8. Numerical result $T(t)$ for $N = 8$ and $\alpha = 1$ in $[0, 1]$.

Table 2. Numerical results comparison for $I(t)$.

Method	$t = 0.4$	$t = 0.6$	$t = 0.8$	$t = 1.0$
Runge-kutta [5]	$0.131583e-4$	$0.212237e-4$	$0.301774e-4$	$0.400378e-4$
MVIM [14]	$0.131583e-4$	$0.212233e-4$	$0.301745e-4$	$0.400254e-4$
VIM [14]	$0.131487e-4$	$0.210141e-4$	$0.279513e-4$	$0.243156e-4$
LADM-Pade [22]	$0.131591e-4$	$0.212683e-4$	$0.300691e-4$	$0.398736e-4$
Bessel [32]	$0.129355e-4$	$0.203526e-4$	$0.283730e-4$	$0.369084e-4$
SDCPM	$0.131583e-4$	$0.212237e-4$	$0.301773e-4$	$0.400377e-4$

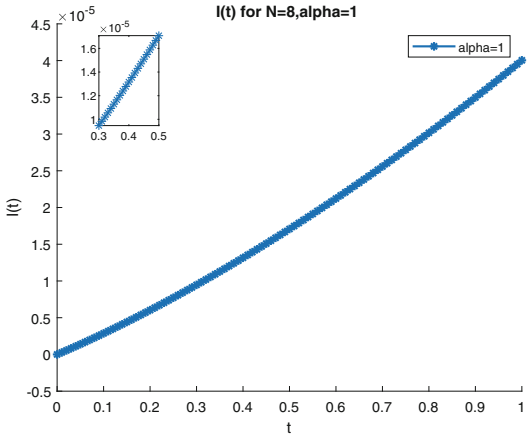

Fig. 9. Numerical result $I(t)$ for $N = 8$ and $\alpha = 1$ in $[0, 1]$.

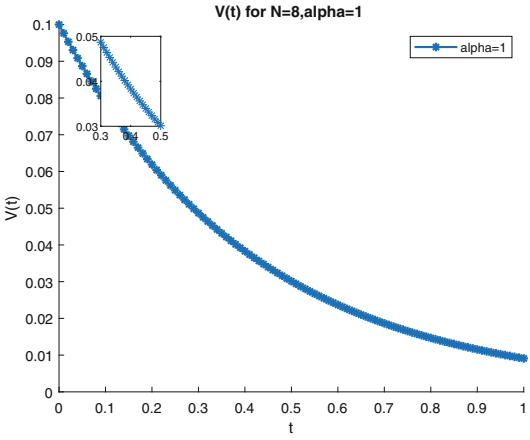

Fig. 10. Numerical result $V(t)$ for $N = 8$ and $\alpha = 1$ in $[0, 1]$.

Table 3. Numerical results comparison for $V(t)$.

Method	$t = 0.2$	$t = 0.4$	$t = 0.6$	$t = 0.8$	$t = 1.0$
Runge-kutta [5]	0.061879	0.038294	0.023704	0.014680	0.009100
MVIM [14]	0.061879	0.038295	0.023710	0.014700	0.009157
VIM [14]	0.061879	0.038308	0.023920	0.016217	0.016084
LADM-Pade [22]	0.061879	0.038313	0.024391	0.009967	0.003305
Bessel [32]	0.061879	0.038294	0.023704	0.014679	0.023704
SDCPM	0.061879	0.038294	0.023704	0.014680	0.009100

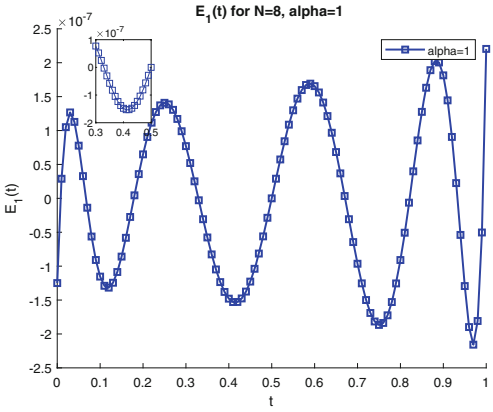

Fig. 11. Error function of $E_1(t)$ for $N = 8$ and $\alpha = 1$.

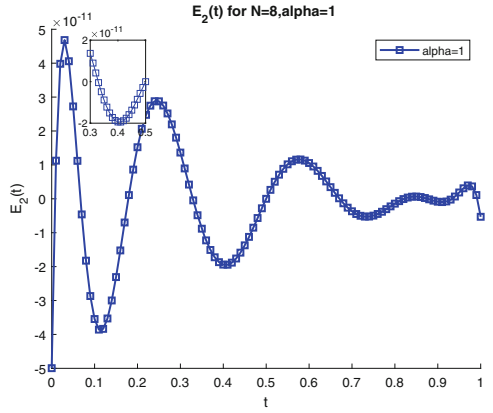

Fig. 12. Error function of $E_2(t)$ for $N = 8$ and $\alpha = 1$.

$CD4^+T$ cells infected by the HIV increases significantly for $N = 8$, and $V(t)$, the number of free HIV particles in the blood decrease in a very short time after infection.

For $N = 8$ and $\alpha = 1$, Figs. 11, 12, and 13 display the error functions obtained with an accuracy of the solutions by utilizing the mentioned strategy given by Eqs. (20). The numerical values of the approximate solutions $T(t)$, $I(t)$, and $V(t)$ of the present method for $N = 8$ in the interval $[0, 1]$ are compared with the Legendre Wavelet Collocation strategy [5], the Runge-Kutta strategy [5], the variational iteration strategy [14], the modified variational iteration strategy [14], the Laplace Adomian decomposition-pade strategy [22] and the Bessel collocation [32] in Tables 1, 2, and 3. To comparison of error functions provided by Eqs. (20) for $T(t)$, $I(t)$, and $V(t)$ of the current method for $N = 8$ in the interval $[0, 1]$ are reported in Tables 4, 5, and 6. These results lead to the conclusion that

the numerical solutions of the present method are better than those obtained with other methods since the absolute errors have gotten by the current strategy are superior to other methods.

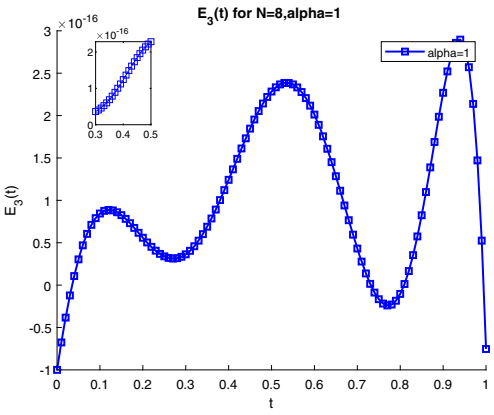

Fig. 13. Error function of $E_3(t)$ for $N = 8$ and $\alpha = 1$.

Table 4. Comparison error results for $T(t)$.

Method	$t = 0.2$	$t = 0.4$	$t = 0.6$	$t = 0.8$	$t = 1.0$
LWCM [5]	$7.50e-06$	$2.70e-05$	$7.34e-05$	$1.77e-04$	$3.98e-04$
MVIM [14]	$7.85e-05$	$3.00e-04$	$8.49e-04$	$2.14e-03$	$5.14e-03$
VIM [14]	$7.78e-05$	$1.94e-04$	$1.13e-03$	$1.41e-02$	$8.00e-02$
LADM-Pade [22]	$7.77e-05$	$1.65e-04$	$2.43e-03$	$3.46e-02$	$2.58e-01$
Bessel [32]	$4.87e-03$	$2.56e-02$	$6.81e-02$	$1.36e-01$	$2.04e-01$
SDCPM	$6.48e-08$	$1.47e-07$	$1.65e-07$	$9.09e-08$	$2.20e-07$

Table 5. Comparison error results for $I(t)$.

Method	$t = 0.2$	$t = 0.4$	$t = 0.6$	$t = 0.8$	$t = 1.0$
LWCM [5]	$8.36e-10$	$1.95e-09$	$3.20e-09$	$4.63e-09$	$6.44e-09$
MVIM [14]	$1.19e-09$	$5.29e-09$	$1.27e-08$	$2.27e-08$	$3.12e-08$
VIM [14]	$1.12e-09$	$4.23e-09$	$1.96e-07$	$2.20e-06$	$1.57e-05$
LADM-Pade [22]	$1.20e-09$	$6.15e-09$	$5.78e-08$	$8.26e-08$	$1.21e-07$
Bessel [32]	$2.16e-07$	$2.17e-07$	$8.58e-07$	$1.78e-06$	$3.09e-06$
SDCPM	$1.52e-11$	$1.94e-11$	$1.05e-11$	$1.42e-12$	$5.30e-12$

Table 6. Comparison error results for $V(t)$.

Method	$t = 0.2$	$t = 0.4$	$t = 0.6$	$t = 0.8$	$t = 1.0$
LWCM [5]	$1.00e-10$	$1.24e-06$	$1.15e-06$	$9.50e-07$	$7.61e-07$
MVIM [14]	$5.61e-08$	$1.06e-06$	$5.75e-06$	$2.01e-05$	$5.64e-05$
VIM [14]	$1.00e-07$	$1.33e-05$	$2.16e-04$	$1.54e-03$	$6.98e-03$
LADM-Pade [22]	$1.08e-07$	$1.84e-05$	$6.87e-04$	$4.71e-03$	$5.80e-03$
Bessel [32]	$6.59e-08$	$3.79e-08$	$2.31e-07$	$7.87e-07$	$1.46e-02$
SDCPM	$2.06e-16$	$9.64e-17$	$6.47e-17$	$2.12e-16$	$8.01e-17$

7 Conclusion

This research looked at the design of protein-protein interaction (PPI) networks and compared them to each other as well. Besides, the mathematical model of fractional HIV infection of $CD4^+T$ cells was introduced, which refers to a class of nonlinear differential equation structures. The SDCPM was suggested for finding approximate solutions to the HIV infection model of $CD4^+T$ cells. With the help of an example, the precision and reliability of the current procedure were illustrated. All calculations were done with the aid of a Maple 17 computer program.

References

1. Ali, N., Ahmad, S., Aziz, S., Zaman, G.: The adomian decomposition method for solving HIV infection model of latently infected cells. Matrix Sci. Math. **3**, 5–8 (2019)
2. Anastasio, T.J.: The fractional-order dynamics of bainstem vestibulo-oculomotor neurons. Biol. Cybern. **72**, 69–79 (1994)
3. Angulo, J., Cuesta, T., Menezes, E., Pedroso, C., Brites, C.: A systematic review on the influence of HLA-B polymorphisms on HIV-1 mother to child transmission. Braz. J. Infec. Dis. **23**, 53–9 (2019)
4. Asquith, B., Bangham, C.R.M.: The dynamics of T-cell fratricide: application of a robust approach to mathematical modelling in immunology. J. Theoret. Biol. **222**, 53–69 (2003)
5. Attaullah, Sohaib, M.: Mathematical modeling and numerical simulation of HIV infection model. Results Appl. Math. **7**, 100–118 (2020)
6. Conte, D., Farsimadan, E., Moradi, L., Palmieri, F., Paternoster, B.: Time-Delay Fractional Optimal Control Problems: A Survey Based on Methodology. In: Proceedings of the 8th International Conference on Fracture, Fatigue and Wear, Belgium, pp. 325–337 (2021)
7. Djordjević, V.D., Jarić, J., Fabry, B., Fredberg, J.J., Stamenović, D.: Fractional derivatives embody essential features of cell rheological behavior. Ann. Biomed. Eng. **31**, 692–699 (2003)
8. Duro, R., Pereira, N., Figueiredo, C., Pineiro, C., Caldas, C., Serrao, R.: Routine CD4 monitoring in HIV patients with viral suppression: is it really necessary? A Portuguese cohort. J. Microbiol. Immunol. Infect. **51**, 593–7 (2018)

9. Gogin, N., Hirvensalo, M.: On the generating function of discrete Chebyshev polynomials. J. Math. Sci. **2**, 224 (2017)
10. Kirschner, D.E.: Using mathematics to understand HIV immune dynamics. Not. Am. Math. Soc. **43**, 191–202 (1996)
11. Hallbergc, D., Kimariob, T., Mtuyab, C., Msuyab, M., Bjorlingc, G.: Factors affecting HIV disclosure among partners in morongo. tanzania. Int J Afr Nurs Sci 10, 49–54 (2019)
12. Jesus, I.S., Machado, J.A.T., Cunha, J.B.: Fractional electrical impedances in botanical elements. J. Vib. Control **14**, 1389–1402 (2008)
13. Li, Q., Xiao, Y.: Global dynamics of a virus immune system with virus guided therapy and saturation growth of virus. Math. Probl. Eng. 1–18 (2018)
14. Merdan, M., Gökdogan, A., Yildirim, A.: On the numerical solution of the model for HIV infection of CD4+T-cells. Comput. Math. Appl. **62**, 118–123 (2011)
15. Moradi, L., Mohammadi, F.: A comparative approach for time-delay fractional optimal control problems: discrete versus continuous Chebyshev polynomials. Asian J. Control **21**(6), 1–13 (2019)
16. Nelson, P.W., Perelson, A.S.: Mathematical analysis of delay differential equation models of HIV-1 infection. Math. Biosci. **179**, 73–94 (2002)
17. Nigmatullin, R.R., Nelson, S.O.: Recognition of the fractional kinetics in complex systems: dielectric properties of fresh fruits and vegetables form 0.01 to 1.8 GHz. Signal Process. **86**, 2744–2759 (2006)
18. Nikiforov, A.F., Suslov, S.K., Uvarov, V.B.: Classical Orthogonal Polynomials of a Discrete Variable. Springer Series in Computational Physics, Springer, Heidelberg (1991). https://doi.org/10.1007/978-3-642-74748-9_2
19. Nowak, M., May, R.: Mathematical biology of HIV infections: antigenic variation and diversity threshold. Math. Biosci. **106**, 1–21 (1991)
20. Oldham, K.B., Spanier, J.: The Fractional Calculus. Academic Press, New York (1974)
21. Omondi, E., Mbogo, W., Luboobi, L.: A mathematical modeling study of HIV infection in two heterosexual age groups in Kenya. Infec. Dis. Modell. **4**, 83–98 (2019)
22. Ongun, M.: The Laplace adomian decomposition method for solving a model for HIV infection of CD4+T-cells. Math. Comput. Modell. **63**, 597–603 (2011)
23. Perelson, A.S., Kirschner, D.E., Boer, R.D.: Dynamics of HIV infection CD4$^+$T cells. Math. Biosci. **114**, 81–125 (1993)
24. Perelson, A.S., Nelson, P.W.: Mathematical analysis of HIV-I dynamics in vivo. SIAM Rev. **41**(1), 3–44 (1999)
25. Petrovic, L.M., Spasic, D.T., Atanackovic, T.M.: On a mathematical model of a human root dentin. Dent. Mater. **21**, 125–128 (2005)
26. Ransome, Y., Thurber, K., Swen, M., Crawford, N., Germane, D., Dean, L.: Social capital and HIV/AIDS in the United States: knowledge, gaps, and future directions. SSM Popul. Health **5**, 73–85 (2018)
27. Riordan, J.: An Introduction to Combinatorial Analysis. Wiley, New York (1980)
28. Samko, S.G., Kilbas, A.A., Marichev, O.I.: Fractional Integrals and Derivatives: Theory and Applications. Gordon and Breach, Langhorne (1993)
29. Theys, K., Libin, P., Pena, A.C.P., Nowe, A., Vandamme, A.M., Abecasis, A.B.: The impact of HIV-1 within host evolution on transmission dynamics. Curr. Opin. Virol. **28**, 92–101 (2018)
30. Wang, L., Li, M.Y.: Mathematical analysis of the global dynamics of a model for HIV infection of CD4+T cells. Math. Biosci. **200**, 44–57 (2006)

31. Yddotuzbasi, S., Karacayir, M.: An exponential Galerkin method for solution of HIV infected model of CD4+t-cells. Comput. Biol. Chem. **67**, 205–12 (2017)
32. Yüzbas, S.: A numerical approach to solve the model for HIV infection of CD4+T-cells. Appl. Math. Model. **36**, 5876–5890 (2012)